BEAM PROFILE MEASUREMENTS FOR MAGNETIZED HIGH ENERGY COOLING DEVICES

T. Weilbach, K. Aulenbacher, M. Bruker, Helmholtz-Institut Mainz, Germany

Abstract

Recent developments in the field of high intensity electron beams in the regime below 10 MeV, e.g. energy recovery linacs or magnetized high energy electron coolers [1], have led to special demands on the beam diagnostics. Since commonly used diagnostic tools like synchrotron radiation and scintillation screens are ineffective or not able to withstand the beam power without being damaged, new methods are needed. Hence a beam profile measurement system based on beam induced fluorescence (**BIF**) was built. This quite simple system images the light generated by the interaction of the beam with the residual gas onto a PMT. A more elaborated system, the Thomson Laser Scanner (**TLS**) — the non-relativistic version of the Laser Wire Scanner — is proposed as a method for non-invasive measurement of all phase space components, especially in the injector and merger parts of an ERL. Both methods are implemented in a 100 keV photo gun.

INTRODUCTION

The new high energy cooling devices easily reach several MWs of beam power. Due to high voltage breakdowns and the energy recuperation in the collector, they allow only a very small beam loss, which is not compatible with normal destructive diagnostics.

There are already several non-destructive beam diagnostic methods established, which are used in different accelerators, such as a scintillation profile monitor [2] at COSY, [3] at GSI or the laser wire scanner at the synchrotron source PETRA III [4]. These methods can be adapted for the profile measurement of high intensity electron beams.

BEAM INDUCED FLUORESCENCE

For protons and ions, beam profile measurement based on beam induced fluorescence is a common technique [5]. The idea is to image the fluorescing residual gas on a photo detector with a spatial resolution. Instead of a detector with a spatial resolution, a photomultiplier tube (PMT) with a slit in front of it can be used. The slit cuts out a small slice of the electron beam image at the PMT as indicated in Fig. 1. By moving the slit up and down, a beam profile can be measured.

To measure the beam induced fluorescence, a new vacuum chamber has been installed at the polarized test source (PKAT) [6] shown in Fig. 2 at the Mainzer Mikrotron (MAMI). In this source, a NEA-GaAs [7] photo cathode is used, which requires a pressure much lower than 10^{-10} mbar for stable operation. Therefore, this chamber is separated from the cathode chamber by two differential pumping stages. The first one consists of a turbo molecular pump (purple) and the second one of two ion getter pumps (blue). This allows local pressure bumps of up to 10^{-5} mbar while maintaining the XHV condition at the cathode. These high pressures are necessary to achieve a significant amount of fluorescent light because the beam current of the photo gun is limited to a few 100 µA.

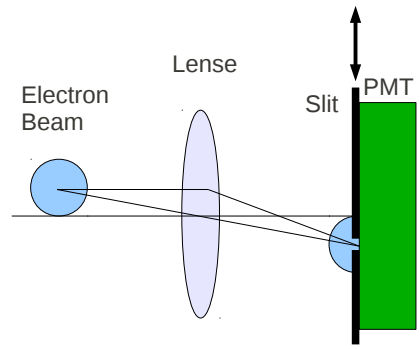

Figure 1: Schematic view of the beam induced fluorescence profile measurement done with a PMT and a slit.

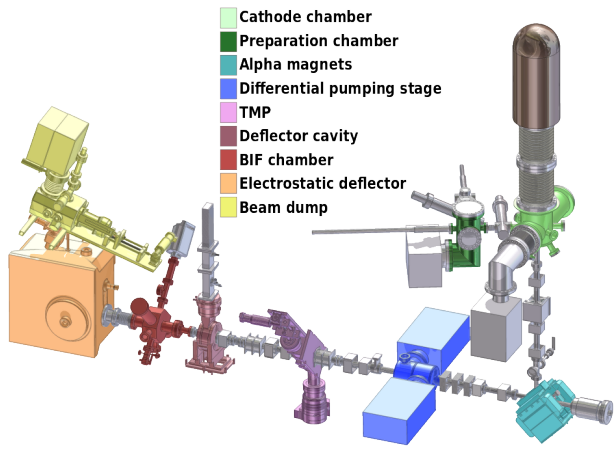

Figure 2: The polarized test source PKAT.

With this setup, first beam profiles have been measured. The conditions during the measurement are listed in Table 1. Since the light yield scales linearly with pressure and current, these conditions are comparable to the conditions in an electron cooling device. There a residual gas pressure of 10^{-9} mbar in combination with a current of 1 A generates the same amount of photons as in our measurements.

A typical measurement is shown in Fig. 3. In this case the laser was pulsed with a pulswidth of 2 ms and a spacing between the pulses of 20 ms. The resulting duty factor of 0.1 and the average beam current of 50 µA measured at the beam dump results in a peak current of 500 µA. A convolu-

ISBN 978-3-95450-140-3

Table 1: BIF Profile Measurement Conditions

Beam energy	100 keV
Beam current	100 µA
Residual gas pressure	$\approx 10^{-5}$ mbar
PMT voltage	1000 V
Slit width	0.2 mm

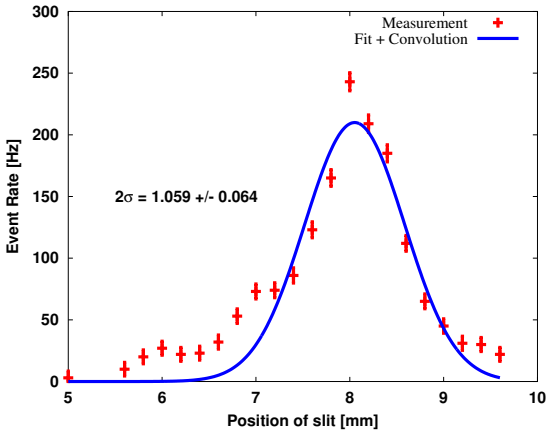

Figure 3: Beam profile measurement with subtracted background.

tion of a Gaussian function and a slit function is fit with a least square fit to provide the beam size. The background, mainly dominated by thermally generated photoelectrons in the PMT, is already subtracted in Fig. 3.

The signal to noise ratio during these measurement was ≈ 1. The thermal background will be insignificant during TLS measurements since it is uncorrelated to the pulsed photon beam, in addition, can be reduced by several orders of magnitude by cooling of the PMT. Since electron beam induced background was negligible, with respect to the thermal background so far, this sets an upper limit for the expectable background. Experiments in the near future will reveal the real background conditions.

THOMSON SCATTERING

Thomson scattering describes elastic scattering of a photon on a free electron. It is the low energy limit of the Compton scattering process. Figure 4 shows a schematic view of Thomson scattering.

A photon λ_L hits the electron beam with an angle Θ and is scattered with the scattering angle Θ'. The scattered photon λ_S gains energy due to the Doppler shift. The wavelength of the scattered photon as a function of the angle between incident photon and electron and the angle between scattered photon and electron and can be evaluated with

$$\lambda_S = \lambda_L \frac{(1+\beta\cos\Theta')}{(1+\beta\cos\Theta)} \quad (1)$$

where β is the electron velocity in units of the speed of

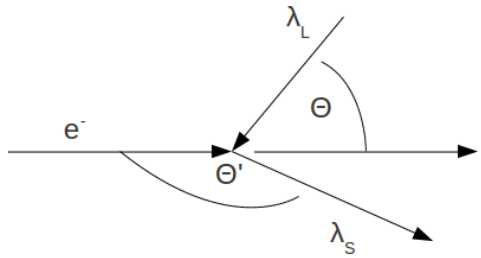

Figure 4: Thomson scattering scheme.

Table 2: Scattering Rate for Different Cooling Devices

Beam energy	$\lambda_L/\mu m$	λ_S/nm	Event rate $/s^{-1}$
100 keV (PKAT)	1.03	630	14
2 MeV (COSY)	10.6	220	$6.1 \cdot 10^2$
4.5 MeV (HESR)	10.6	50	$1.2 \cdot 10^3$
8 MeV (ENC)	10.6	20	$2.1 \cdot 10^3$

light. The scattering process is determined by the Thomson cross section

$$\frac{d\sigma}{d\Omega} = \frac{1}{2} r_e^2 \left(1 + \cos^2\Theta'\right) \quad (2)$$

with r_e = classical electron radius. The number of scattered photons can be calculated with the following equation

$$R = \frac{1}{2} r_e^2 (1 + cos^2(\Theta') N_L n_e P \epsilon \Delta\Omega l \frac{(1+\beta cos(\Theta))}{(1+\beta cos(\Theta'))\gamma} \quad (3)$$

with N_L = Number of incident photons per Joule, n_e = Electron density, P = laser power, ϵ = Detector system efficiency, $\Delta\Omega$ = Detector solid angle, l = Interaction length, $\frac{(1+\beta\cos(\Theta))}{(1+\beta\cos(\Theta'))\gamma}$ = factor results from Lorentz transformation.

Beam Diagnostics

For our experiment, we are using the following angles: $\Theta = 90°$ and $\Theta' = 135°$ or $\Theta' = 180°$, respectively. In this case, the rate of the scattered photons only depends on the electron density in the electron beam. By moving the laser beam through the electron beam, a profile measurement can be done. Due to the low cross section, which is mostly dominated by the classical electron radius squared, the required laser power is very high. This was the reason why the pioneer experiment done in 1987/88 suffered from very low count rates [8, 9]. With the development in laser technology, it is now possible to achieve higher count rates, which makes this method interesting. In Table 2 the event rates for different setups are shown. For the calculation, a 100 W laser system and an electron beam current of 1 A and a diameter of 3 cm was chosen. The detector system efficiency is estimated to be $\epsilon = 0.2$ and solid angle $\Delta\Omega = 100$ msr.

The TLS measurements the PKAT has to be modified. Recently, these modifications have been carried out as shown in Fig. 5. The electrostatic deflector was replaced

ISBN 978-3-95450-140-3

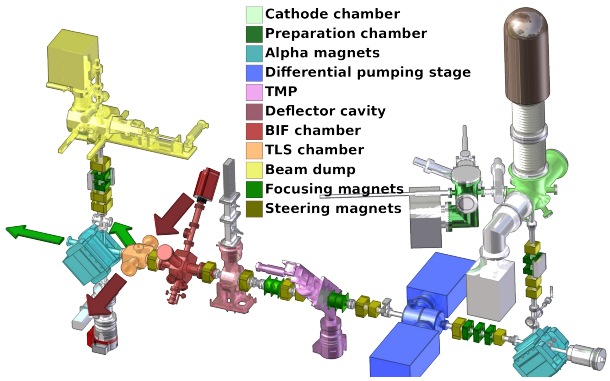

Figure 5: The PKAT after the modifications. The red arrows indicate the IR-laser light and the green arrows the two possible positions to detect the scattered photons ($\Theta' = 135°$ and $\Theta' = 180°$).

Table 3: Laser System Specifications

	Green	IR
Wavelength	516 nm	1032 nm
Power	10 W	150 W
Pulse duration	20 ns	20 ns
Rep. rate	150 kHz	150 kHz

with an alpha magnet and a new TLS chamber was installed. This enables a detection of the scattered photons in two different positions ($\Theta' = 135°$ and $\Theta' = 180°$) while the electrons are bent by 270°. To focus the beam into the beam dump, a quadrupole doublet was also added to the beam line as well as new steering magnets. This should help to decrease the background created by beam losses at the wall of the vacuum chamber. To achieve the desired electron beam density for the event rates mentioned above, we need an electron beam with a current of 100 mA and a diameter of 3 mm.

The Laser System

The power supply of the PKAT is capable of delivering 3 mA of beam current so the required 100 mA can only be achieved in a pulsed mode. Therefore, a new laser system was purchased. It consists of a green laser to create the electron beam at the photo cathode and a IR laser for the Thomson scattering. The parameters of the laser system are shown in Tab. 3. In this case, a system with a high repetition frequency was chosen to lower the peak power of the laser to stay below the damage threshold of the different components, e.g. vacuum windows. This in combination with the pulse duration gives a duty cycle of $2 \cdot 10^{-3}$, i.e. despite of the 100 mA peak current, the average beam current is only 200 µA. This keeps the beam power low, and there is no need of a special beam dump capable of handling several kW of beam power.

Since the count rate suffers from the low cross section of the Thomson scattering, the timing between electron and laser beam is essential for this experiment. If laser and electron beam are not synchronized very carefully, the count rate in the detector decreases enormously due to the low electron density or the lower number of photons in the scattering process. Therefore, a synchronization unit can delay one laser with respect to the other by up to 1000 ns in steps of 1 ns so the time the electrons need to travel from the source to the TLS-chamber can be compensated for.

OUTLOOK

To increase the dynamic range and the signal to noise ratio of the BIF measurements, a cooling system for the PMT will be installed. In this setup more detailed background studies will be carried out. Also, a YAG screen was installed in the BIF chamber, and we are planning to do beam profile measurements with both methods to compare the results.

The installation of both lasers including enclosure for safety issues should be finished shortly. For beam profile measurements, a system which is able to displace the laser beam will be installed in the future.

REFERENCES

[1] T. Bergmark et al., "Status of the HESR Electron Cooler Design Work", TUPLS067, Proceedings of EPAC 2006, Edinburgh, Scotland.

[2] C. Boehme et al., "Gas Scintillation Beam Profile Monitor at COSY Jülich", TUPSM005, Proceedings of BIW 2010, Santa Fee, New Mexico USA.

[3] F. Becker et al., "Beam Induced Fluorescence Monitor-Spectroscopy in Nitrogen, Helium, Argon, Krypton, and Xenon Gas", TUPSM020, Proceedings of BIW 2010, Santa Fee, New Mexico USA.

[4] M.T. Price et al., "Beam Profile Measurements with the 2-D Laser-Wire Scanner at PETRA", FRPMN094, Proceedings of PAC 2007, Albuquerque, New Mexico USA.

[5] F. Becker, "Beam Induced Fluorescence Monitors", WEOD01, Proceedings of DIPAC 2011, Hamburg, Germany.

[6] P. Hartmann: "Aufbau einer gepulsten Quelle polarisierter Elektronen", Dissertation 1997, JGU Mainz, Germany

[7] D.T. Pierce et al., Appl. Phys. Lett. 26 (1975) 670.

[8] C. Habfast et al., "Measurement of Laser Light Thomson-Scattered from a Cooling Electron Beam", Appl. Phys. B 44, 87-92 (1987).

[9] J. Berger et al.: Thomson Scattering of Laser Light from a Relativistic Electron Beam, Physica Scripta. Vol. T22, 296-299, 1988.

ISBN 978-3-95450-140-3